

Demixing of colloid-polymer mixtures in poor solvents

Matthias Schmidt* and Alan R. Denton

Department of Physics, North Dakota State University, Fargo, North Dakota 58105-5566

(Received 8 March 2002; published 26 June 2002)

The influence of poor solvent quality on fluid demixing of a model mixture of colloids and nonadsorbing polymers is investigated using density functional theory. The colloidal particles are modeled as hard spheres and the polymer coils as effective interpenetrating spheres that have hard interactions with the colloids. The solvent is modeled as a two-component mixture of a primary solvent, regarded as a background theta solvent for the polymer, and a cosolvent of point particles that are excluded from both colloids and polymers. Cosolvent exclusion favors overlap of polymers, mimicking the effect of a poor solvent by inducing an effective attraction between polymers. For this model, a geometry-based density functional theory is derived and applied to bulk fluid phase behavior. With increasing cosolvent concentration (worsening solvent quality), the predicted colloid-polymer demixing binodal shifts to lower colloid concentrations, promoting demixing. For sufficiently poor solvent, a reentrant demixing transition is predicted at low colloid concentrations.

DOI: 10.1103/PhysRevE.65.061410

PACS number(s): 82.70.Dd, 61.20.Gy, 64.10.+h, 64.60.Fr

I. INTRODUCTION

Solvents play a crucial role in the thermodynamic behavior of macromolecular solutions. Over the past half a century, effects of solvent quality on the physical properties of polymer solutions have been extensively studied [1,2]. Polymer-solvent and solvent-solvent interactions were first incorporated into the classic Flory-Huggins mean-field theory of polymer solutions [3]. Subsequently, excluded-volume interactions between polymer segments were identified as the key determinants of solvent quality. Polymer segments sterically repel one another in a good solvent, attract in a poor solvent, and behave as though nearly ideal (noninteracting) in a theta solvent. Interactions between polymer segments strongly influence chain conformations and, in turn, phase separation and other macroscopic phenomena.

Compared to solvent effects in pure polymer solutions, much less is known about the role of solvent quality in colloid-polymer mixtures. The simplest and most widely studied theoretical model of colloid-polymer mixtures is the Asakura-Oosawa (AO) model [4,5]. This treats the colloids as hard spheres and the polymers as effective spheres that are mutually noninteracting but have hard interactions with the colloids. The thermodynamic phase diagram of the AO model has been mapped out by thermodynamic perturbation theory [6], free volume theory [7], density functional (DF) theory [8], and Monte Carlo simulation [9]. By assuming ideal polymers, however, the AO model is implicitly limited to theta solvents. Recently, by incorporating polymer-polymer repulsion into the AO model, the influence of a good solvent on phase behavior has been explored via perturbation theory [10] and DF theory [11]. All of these studies assume an effective penetrable-sphere model for the polymer coils, which is supported by explicit Monte Carlo simulations of interacting segmented-chain polymers [12–14]. An

alternative, more microscopic, theoretical approach is the PRISM integral-equation theory [15], which models polymers on the segment level.

The purpose of the present paper is to investigate the effect of a *poor* solvent on the bulk phase behavior of colloid-polymer mixtures. To this end, we consider a variation of the AO model that explicitly includes the solvent as a distinct component. Specifically, the solvent is treated as a binary mixture of a primary solvent, which alone acts as a theta solvent for the polymer, and a cosolvent, which acts as a poor solvent for the polymer. The primary solvent is regarded as a homogeneous background that freely penetrates the polymer, but is excluded by the colloids. The cosolvent is modeled simply as an ideal gas of pointlike particles that penetrate neither colloids nor polymers.

In the absence of colloids, the polymer-cosolvent subsystem is the Widom-Rowlinson (WR) model of a binary mixture [16,17], in which particles of unlike species interact with hard cores and particles of like species are noninteracting. The WR model can be shown to be equivalent to a one-component system of penetrable spheres that interact via a many-body interaction potential, proportional to the cosolvent pressure and the volume covered by the spheres (with overlapping portions counted only once). Hence, in the polymer-cosolvent subsystem, the volume occupied by the polymer spheres costs interaction energy, inducing an effective attraction between polymers reminiscent of that caused by a poor solvent. By varying cosolvent concentration, the solvent quality can be tuned. Here we investigate whether and how added hard colloidal spheres mix with such effectively interacting polymers.

In Sec. II, we define more explicitly the model colloid-polymer-cosolvent mixture. In Sec. III, we develop a general geometry-based DF theory, which may be applied to both homogeneous and inhomogeneous states of the model system. The general theory provides the foundation for an application to bulk phase behavior in Sec. IV. Readers who are interested only in bulk properties may wish to skip Sec. III and turn directly to Sec. IV. We finish with concluding remarks in Sec. V.

*Permanent address: Institut für Theoretische Physik II, Heinrich-Heine-Universität Düsseldorf, Universitätsstraße 1, D-40225 Düsseldorf, Germany.

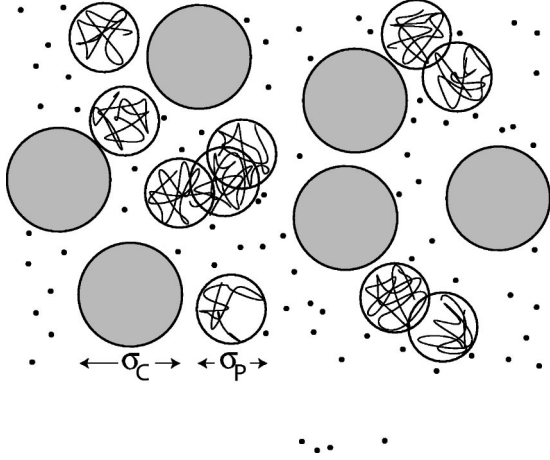


FIG. 1. Model ternary mixture of colloidal hard spheres of diameter σ_C , polymer effective spheres of diameter σ_P , and pointlike solvent particles.

II. THE MODEL

We consider a ternary mixture of colloidal hard spheres (species C) of radius R_C , globular polymers (species P) of radius R_P , and pointlike cosolvent particles (species S), as illustrated in Fig. 1. The respective number densities are $\rho_C(\mathbf{r})$, $\rho_P(\mathbf{r})$, and $\rho_S(\mathbf{r})$, where \mathbf{r} is the spatial coordinate. The primary solvent is regarded as a homogeneous background for the polymer and is not explicitly included. All particles experience only pairwise interactions, $V_{ij}(r)$, $i, j = C, P, S$, where r is the separation distance between particle centers. Colloids behave as hard spheres: $V_{CC}(r) = \infty$, if $r < 2R_C$, and zero otherwise. Colloids and polymers interact as hard bodies via $V_{CP}(r) = \infty$, if $r < R_C + R_P$, and zero otherwise, and both exclude cosolvent particles: $V_{CS}(r) = \infty$, if $r < R_C$, $V_{PS}(r) = \infty$, if $r < R_P$, and zero otherwise. The polymers and cosolvent particles behave as ideal gases: $V_{PP}(r) = 0$, $V_{SS}(r) = 0$, for all r . In essence, this is the AO model with additional point particles that cannot penetrate either colloids or polymers.

We denote the sphere diameters by $\sigma_C = 2R_C$ and $\sigma_P = 2R_P$, the bulk packing fractions by $\eta_C = 4\pi R_C^3 \rho_C / 3$ and $\eta_P = 4\pi R_P^3 \rho_P / 3$, and define a dimensionless solvent bulk density $\rho_S^* = \rho_S \sigma_P^3$. The polymer-colloid size ratio $q = \sigma_P / \sigma_C$ is regarded as a control parameter.

$$\Phi_C = -n_0^C \ln(1 - n_3^C) + \frac{n_1^C n_2^C - \mathbf{n}_{v1}^C \cdot \mathbf{n}_{v2}^C}{1 - n_3^C} + \left[\frac{1}{3} (n_2^C)^3 - n_2^C (\mathbf{n}_{v2}^C)^2 + \frac{3}{2} (\mathbf{n}_{v2}^C \cdot \hat{\mathbf{n}}_{m2}^C \cdot \mathbf{n}_{v2}^C - 3 \det \hat{\mathbf{n}}_{m2}^C) \right] / [8\pi(1 - n_3^C)^2]. \quad (6)$$

The colloid-polymer interaction contribution Φ_{CP} is the same as in the pure AO case [8],

$$\Phi_{CP} = \sum_{\nu} \frac{\partial \Phi_C}{\partial n_{\nu}^C} n_{\nu}^P, \quad (7)$$

III. DENSITY FUNCTIONAL THEORY

We develop a geometry-based DF theory for the excess Helmholtz free energy of the model system, expressed as an integral over an excess free energy density,

$$F_{\text{exc}}[\rho_C, \rho_P, \rho_S] = k_B T \int d^3x \Phi(\{n_{\nu}^i\}), \quad (1)$$

where k_B is Boltzmann's constant, T is absolute temperature, and the (local) reduced excess free energy density Φ is a simple function (not a functional) of weighted densities n_{ν}^i . The weighted densities are smoothed averages of the possibly highly inhomogeneous density profiles $\rho_i(\mathbf{r})$ expressed as convolutions,

$$n_{\nu}^i(\mathbf{r}) = \rho_i(\mathbf{r}) * w_{\nu}^i(\mathbf{r}) = \int d\mathbf{r}' \rho_i(\mathbf{r}') w_{\nu}^i(\mathbf{r} - \mathbf{r}'), \quad (2)$$

with respect to weight functions $w_{\nu}^i(\mathbf{r})$ where $i = C, P, S$ and $\nu = 0, 1, 2, 3, v1, v2, m2$. The usual weight functions [18,19] are

$$w_2^i(\mathbf{r}) = \delta(R_i - r), \quad w_3^i(\mathbf{r}) = \Theta(R_i - r), \quad (3)$$

$$\mathbf{w}_{v2}^i(\mathbf{r}) = w_2^i(\mathbf{r}) \frac{\mathbf{r}}{r}, \quad \hat{\mathbf{w}}_{m2}^i(\mathbf{r}) = w_2^i(\mathbf{r}) \left(\frac{\mathbf{r}\mathbf{r}}{r^2} - \frac{\hat{\mathbf{1}}}{3} \right), \quad (4)$$

where $r = |\mathbf{r}|$, $\delta(r)$ is the Dirac distribution, $\Theta(r)$ is the step function, and $\hat{\mathbf{1}}$ is the identity matrix. Further linearly dependent weight functions are $w_1^i(\mathbf{r}) = w_2^i(\mathbf{r}) / (4\pi R)$, $\mathbf{w}_{v1}^i(\mathbf{r}) = \mathbf{w}_{v2}^i(\mathbf{r}) / (4\pi R)$, and $w_0^i(\mathbf{r}) = w_1^i(\mathbf{r}) / R$. The weight functions for $\nu = 3, 2, 1, 0$ represent geometrical measures of the particles in terms of volume, surface area, integral mean curvature, and Euler characteristic, respectively [18]. Note that the weight functions differ in tensorial rank: w_0^i , w_1^i , w_2^i , and w_3^i are scalars, \mathbf{w}_{v1}^i and \mathbf{w}_{v2}^i are vectors, and $\hat{\mathbf{w}}_{m2}^i$ is a (traceless) matrix.

The excess free energy density can be expressed in the general form

$$\Phi = \Phi_C + \Phi_{CP} + \Phi_{CS} + \Phi_{CPS}, \quad (5)$$

where the four contributions have forms motivated by consideration of the appropriate exact zero-dimensional limits. The colloid contribution Φ_C is the same as that for the pure hard-sphere (HS) system [18,19],

while the colloid-solvent interaction contribution [20] is

$$\Phi_{CS} = -n_0^S \ln(1 - n_3^C). \quad (8)$$

Finally, in order to model the WR-type interaction between

polymers and cosolvent particles in the presence of the colloidal spheres, we assume

$$\Phi_{CPS} = \frac{n_0^S n_3^P}{1 - n_3^C}, \quad (9)$$

which takes into account the volume excluded to the polymer and cosolvent by the colloids.

It is instructive to compare the current theory to geometry-based DF theories previously formulated for two related ternary model systems. One starting point is a ternary AO model that combines a binary HS mixture and one polymer species [21]. Letting the radius of the smaller HS component go to zero, one obtains the cosolvent species. The other starting point is a recently introduced model [22] for a ternary mixture of colloids, polymers, and hard vanishingly thin needles of length L , where the needles are ideal amongst themselves but cannot penetrate the polymers (hard-core interaction). In the limit $L \rightarrow 0$, the needles become identical to the cosolvent particles. We have explicitly checked that the DF theories for both systems reduce to the theory described above, demonstrating the internal consistency of the geometry-based approach.

IV. RESULTS AND DISCUSSION

A. Bulk limit

For bulk fluid phases the density profiles are homogeneous: $\rho_i(\mathbf{r}) = \text{const}$. In this case, the integrations in Eq. (2) are trivial, and simple expressions for the weighted densities can be obtained. Inserting these expressions into the excess free energy density [Eqs. (6)–(9)] yields the bulk excess free energy in analytic form. The HS contribution, which is equal to the Percus-Yevick compressibility (and scaled-particle) result, is given as

$$\Phi_C = \frac{3\eta_C[3\eta_C(2-\eta_C) - 2(1-\eta_C)^2 \ln(1-\eta_C)]}{8\pi R_C^3(1-\eta_C)^2}. \quad (10)$$

The colloid-polymer contribution is equal to that predicted by free volume theory [7], and subsequently rederived by DFT [8],

$$\Phi_{CP} = \frac{\eta_P/(8\pi R_P^3)}{(1-\eta_C)^3} \{3q\eta_C[6(1-\eta_C)^2 + 3q(2-\eta_C-\eta_C^2) + 2q^2(1+\eta_C+\eta_C^2)] - 6(1-\eta_C)^3 \ln(1-\eta_C)\}. \quad (11)$$

This contribution is linear in the polymer density and has a form that arises, as in the original free volume theory [7], from treating the polymers as an ideal gas occupying the free volume between the colloids. The colloid-cosolvent contribution is given by

$$\Phi_{CS} = -\rho_S \ln(1-\eta_C). \quad (12)$$

This contribution can be similarly interpreted as the free energy of an ideal gas in the free volume of the colloids. In this case, however, the ideal gas consists of pointlike cosolvent particles, considerably simplifying the analytical form of the free volume. In fact, by letting $q \rightarrow 0$ in Eq. (11), and identifying species P and S , Φ_{CP} reduces to Φ_{CS} . The remaining contribution couples the densities of all three species, and is given by

$$\Phi_{CPS} = \frac{\rho_S \eta_P}{1-\eta_C}. \quad (13)$$

In the absence of colloids ($\eta_C = 0$), this is equivalent to the mean-field free energy of the WR model. Equation (13) is a nontrivial generalization thereof to the case of nonvanishing η_C . For completeness, the reduced ideal-gas free energy is

$$\Phi_{id} = \sum_{i=C,P,S} \rho_i [\ln(\rho_i \Lambda_i^3) - 1], \quad (14)$$

where the Λ_i are (irrelevant) thermal wavelengths of species i . This puts us in a position to obtain the reduced total free energy density $\Phi_{tot} = \Phi_{id} + \Phi$, of any given fluid state characterized by the bulk densities of the three components and the size ratio q .

B. Phase diagrams

The conditions for phase coexistence are equality of the total pressures p_{tot} and of the chemical potentials μ_i in the coexisting phases. For phase equilibrium between phases I and II, $p_{tot}^I = p_{tot}^{II}$ and $\mu_i^I = \mu_i^{II}$, $i = C, P, S$, yielding four equations for six unknowns (two state points, each characterized by three densities). In our case, a set of analytical expressions is obtained from

$$\frac{p_{tot}}{k_B T} = -\Phi_{tot} + \sum_{i=C,P,S} \rho_i \frac{\partial \Phi_{tot}}{\partial \rho_i} \quad (15)$$

and

$$\mu_i = k_B T \frac{\partial \Phi_{tot}}{\partial \rho_i}, \quad (16)$$

the numerical solution of which is straightforward.

In order to graphically represent the ternary phase diagrams, we choose the system reduced densities, η_C , η_P , and ρ_S^* as basic variables. For given q , these span a three-dimensional (3D) phase space. Each point in this space corresponds to a possible bulk state. Two-phase coexistence is indicated by a pair of points joined by a straight tie line. We imagine controlling the system directly with η_C and η_P , but indirectly via coupling to a cosolvent reservoir, whose chemical potential μ_S tunes the solvent quality. Note that, because the cosolvent is treated as an ideal gas, the reservoir's density is simply proportional to its activity. Thus, the reduced density $\rho_S^* = \exp(\mu_S/k_B T)$ may be equivalently taken as a control parameter, which is equal in coexisting phases. To make contact with Flory-Huggins theory, we are implicitly considering here the case in which the Flory inter-

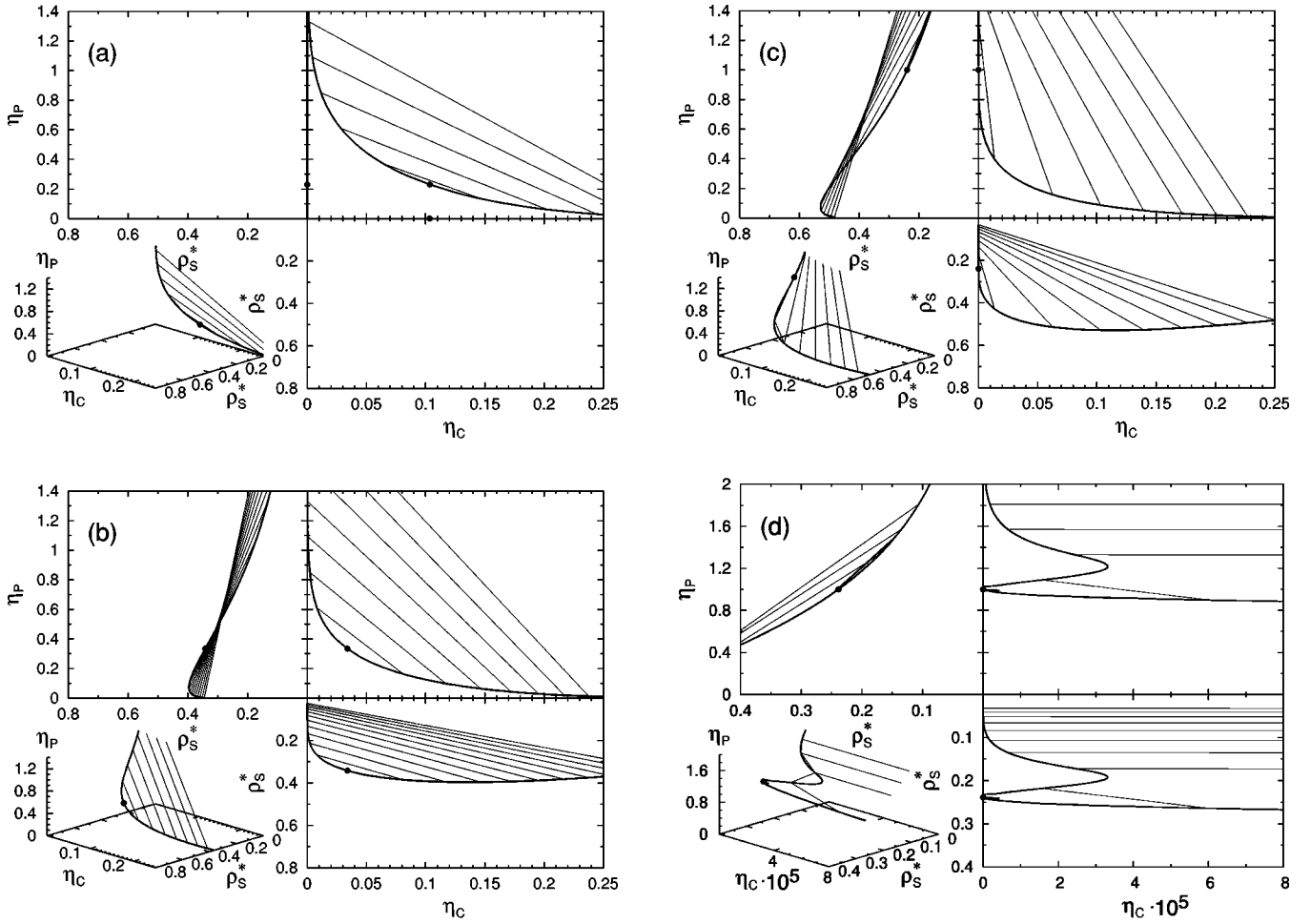


FIG. 2. Demixing phase diagram of the model ternary colloid-polymer-solvent mixture for $\sigma_C = \sigma_P$ and $\rho_S^{*r} = 0$ (a), 0.5 (b), and 0.64894 (c). The latter case is shown also on a finer scale (d).

action parameter χ falls in the range $0.5 < \chi < 1$, corresponding to a negative excluded-volume parameter, $v \propto (1 - 2\chi)$.

We initially consider colloids and polymers of equal size ($\sigma_C = \sigma_P$). For this case, Fig. 2 shows projections of constant- ρ_S^{*r} surfaces onto the three sides of the coordinate system, namely the η_C - ρ_S^* , η_C - η_P , and η_P - ρ_S^* planes, as well as a perspective 3D view. For reference, the phase diagram without cosolvent is shown in Fig. 2(a). This is identical to the common free volume demixing curve of the AO model [7,8]. For $\rho_S^{*r} = 0$, in which case $\rho_S^* = 0$, the η_C - ρ_S^* and η_P - ρ_S^* planes are inaccessible, i.e., all accessible states lie completely within the η_C - η_P plane. Upon increasing the cosolvent reservoir density to $\rho_S^{*r} = 0.5$, and thus worsening the solvent quality, the demixed region grows, as seen in Fig. 2(b). The critical point shifts towards lower η_C and higher η_P , the tie lines become steeper, and the area beneath the colloid-polymer binodal in the η_C - η_P plane (a measure of miscibility) decreases.

As a physical interpretation of the results, one can imagine the polymer spheres as tending to merge (overlap) to avoid contact with the solvent. The resulting polymer “dimers,” “trimers,” etc., act as larger depleting agents, increasing the range of the effective depletion potential be-

tween colloids. At the same time, the lower effective concentration of depletants reduces the osmotic pressure and thus the depth of the potential. Comparing the phase diagrams for different cosolvent reservoir densities, we can conclude that the net effect of merging polymers is to increase the integrated strength of the depletion potential and thus to promote demixing.

Eventually, at $\rho_S^{*r} = 0.64894$, the colloid-polymer critical point meets the η_P - ρ_S^* plane (where $\eta_C = 0$), as seen in Figs. 2(c) and (on a larger scale) 2(d). Polymers and cosolvent here begin to demix already in the absence of colloids (the critical point of the WR model). For still higher cosolvent reservoir densities (beyond the WR critical point), the critical point vanishes from the phase diagram and a polymer-cosolvent miscibility gap opens up at $\eta_C = 0$. It is tempting to interpret this demixing as aggregation of the polymer spheres, although it must be emphasized that the WR model can only crudely describe polymer aggregation.

Another intriguing prediction is the reentrant colloid-polymer mixing evident in Fig. 2(d). For sufficiently low colloid concentrations and high cosolvent reservoir densities (poor solvent), colloids and polymers initially demix with increasing η_P . Upon increasing η_P further, miscibility

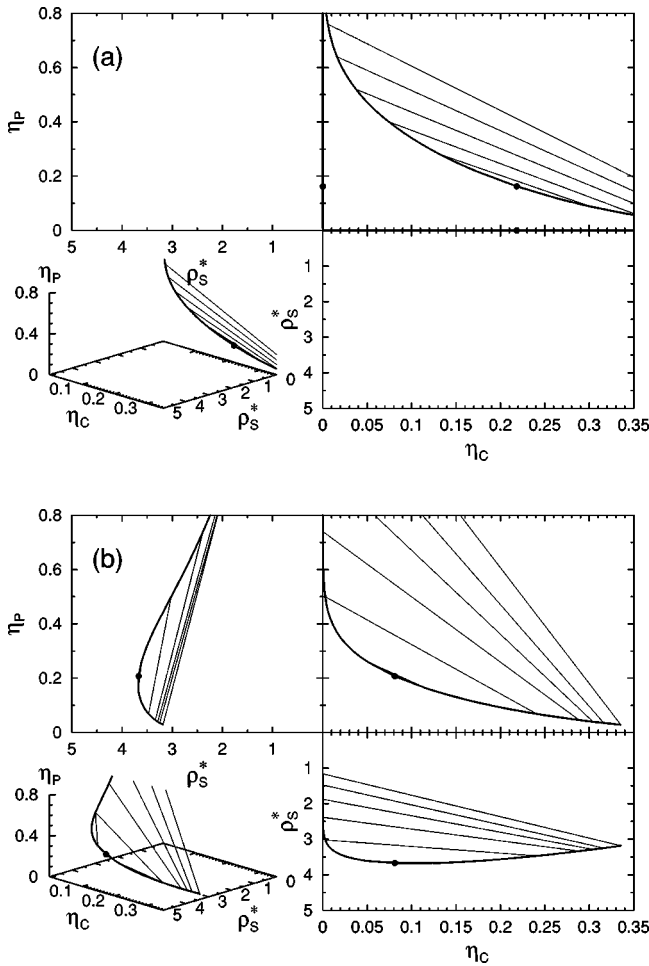


FIG. 3. Same as Fig. 2, but for $\sigma_C = 2\sigma_P$ and $\rho_S^{*r} = 0$ (a) and 0.5 (b).

returns over a small range before demixing again occurs at higher η_P . Such a phenomenon could conceivably result from the complex interplay between range and depth of the depletion potential arising from solvent-induced overlap of polymers.

For smaller polymer-to-colloid size ratios, the above scenario persists. Figure 3 shows qualitatively similar results for $q = 0.5$ and cosolvent reservoir densities $\rho_S^{*r} = 0$ [Fig. 3(a)] and 0.5 [Fig. 3(b)].

V. CONCLUSIONS

In summary, we have investigated the bulk fluid demixing behavior of model mixtures of colloids and nonadsorbing polymers in poor solvents. Our model combines the Asakura-Oosawa model of hard-sphere colloids plus ideal penetrable-sphere polymers with a binary solvent model. The solvent comprises a primary theta solvent and a cosolvent of point particles that are excluded from both colloids and polymers. Cosolvent exclusion energetically favors overlapping configurations of polymers. Although somewhat idealized, the model exhibits the essential feature of solvent-induced effective attraction between polymers, mimicking the effect of a poor solvent.

To study the equilibrium phase behavior of this model, we have derived a geometry-based density functional theory that combines elements of previous theories for the AO and Widom-Rowlinson models. Applying the theory to bulk fluid phases, we have calculated phase diagrams for cosolvent densities spanning a range from theta solvent to poor solvent. With increasing cosolvent concentration (worsening solvent quality), the predicted colloid-polymer binodal shifts to lower colloid concentrations, destabilizing the mixed phase. Beyond a threshold cosolvent concentration, a reentrant colloid-polymer demixing transition is predicted at low colloid concentrations.

Predictions of the theory could be tested by comparison with simulations of the model. Qualitative comparison with experiment also may be possible, but would require a relation between the cosolvent concentration (as a measure of solvent quality) and the Flory interaction parameter. In principle, such a relation could be established by calculating the effective second virial coefficient of the polymer in the polymer-cosolvent subsystem.

Although here we have approximated the polymers as mutually noninteracting, their effective attractions being driven only by cosolvent exclusion, future work should include non-ideality between polymers, arising fundamentally from excluded-volume repulsion between polymer segments. For this purpose, a reasonable model is an effective-sphere description based on a repulsive, penetrable pair interaction (finite at the origin), e.g., of step function or Gaussian shape [12]. The competition between such intrinsic repulsion and the solvent-induced attraction considered in this work is likely to produce rich phase behavior. As a further outlook, our approach also could be applied to effects of solvent quality on polymer brushes adsorbed onto surfaces of colloidal particles.

[1] P. J. Flory, *Statistical Mechanics of Chain Molecules* (Interscience Publishers, New York, 1969).
 [2] P.-G. de Gennes, *Scaling Concepts in Polymer Physics* (Cornell University Press, Ithaca, NY, 1979).
 [3] P. J. Flory, *Principles of Polymer Chemistry* (Cornell University Press, Ithaca, NY, 1971).
 [4] S. Asakura and F. Oosawa, *J. Chem. Phys.* **22**, 1255 (1954).
 [5] A. Vrij, *Pure Appl. Chem.* **48**, 471 (1976).
 [6] A. P. Gast, C. K. Hall, and W. B. Russell, *J. Colloid Interface Sci.* **96**, 251 (1983).

[7] H. N. W. Lekkerkerker, W. C. K. Poon, P. N. Pusey, A. Stroobants, and P. B. Warren, *Europhys. Lett.* **20**, 559 (1992).
 [8] M. Schmidt, H. Löwen, J. M. Brader, and R. Evans, *Phys. Rev. Lett.* **85**, 1934 (2000).
 [9] M. Dijkstra, J. M. Brader, and R. Evans, *J. Phys.: Condens. Matter* **11**, 10079 (1999).
 [10] P. B. Warren, S. M. Ilett, and W. C. K. Poon, *Phys. Rev. E* **52**, 5205 (1995).
 [11] M. Schmidt, A. R. Denton, and J. M. Brader (unpublished).
 [12] A. A. Louis, P. G. Bolhuis, J. P. Hansen, and E. J. Meijer, *Phys.*

- Rev. Lett. **85**, 2522 (2000).
- [13] P. G. Bolhuis, A. A. Louis, J. P. Hansen, and E. J. Meijer, *J. Chem. Phys.* **114**, 4296 (2001).
- [14] P. G. Bolhuis, A. A. Louis, and J. P. Hansen, *Phys. Rev. E* **64**, 021801 (2001).
- [15] S. Ramakrishnan, M. Fuchs, K. S. Schweizer, and C. F. Zukowski, *J. Chem. Phys.* **116**, 2201 (2002).
- [16] B. Widom and J. S. Rowlinson, *J. Chem. Phys.* **52**, 1670 (1970).
- [17] J. S. Rowlinson and B. Widom, *Molecular Theory of Capillarity* (Clarendon Press, Oxford, 1982).
- [18] Y. Rosenfeld, *Phys. Rev. Lett.* **63**, 980 (1989).
- [19] P. Tarazona, *Phys. Rev. Lett.* **84**, 694 (2000).
- [20] M. Schmidt, *Phys. Rev. E* **63**, 050201(R) (2001).
- [21] M. Schmidt, H. Löwen, J. M. Brader, and R. Evans (unpublished).
- [22] M. Schmidt and A. R. Denton, *Phys. Rev. E.* **65**, 021508 (2002).